Pure Appl. Chem., Vol. 84, No. 11, pp. 2325–2337, 2012.
http://dx.doi.org/10.1351/PAC-CON-11-11-03

Identification of heat shock protein 60 as the regulator of the hypoxia-inducible factor subunit HIF-1α*

Hyun Seung Ban, Kazuki Shimizu, Hidemitsu Minegishi, and Hiroyuki Nakamura‡

Department of Chemistry, Faculty of Science, Gakushuin University, Mejiro, Tokyo 171-8588, Japan

Abstract: The hypoxia-inducible factor (HIF) takes part in transcriptional activation of hypoxia-responsive genes such as vascular endothelial growth factor (VEGF), insulin-like growth factor, and inducible nitric oxide synthase. Since VEGF plays an important role in pathological angiogenesis such as tumor growth and ischemic diseases, the inhibition of VEGF inducer HIF is an attractive approach for the inhibition of pathological angiogenesis. Recently, we have reported that the introduction of boronic acid and a carborane moiety into phenoxyacetanilide induced a potent inhibitory effect on HIF-1α activation under hypoxic conditions. In the present study, to clarify the mechanism of action of carboranylphenoxyacetanilide GN26361 against HIF inhibition, we designed and synthesized molecular probes of GN26361 substituted with benzophenone to induce covalent binding with the target protein by UV (photoaffinity labeling) and an acetylenic moiety to conjugate with the green-fluorescent Alexa Fluor 488-azide by click reaction. In-gel fluorescent imaging of target protein bound with the probe was identified as heat shock protein 60 (HSP60). Moreover, direct binding in gel fluorescent imaging was observed by photoaffinity labeling and click reaction of the probe with recombinant HSP60. These results indicate that HSP60 is the target protein of GN26361 and might be a new molecular target for HIF inhibition.

Keywords: anticancer activity; boron; carboranes; chemistry; drug discovery; heat shock protein 60; hypoxia-inducible factor; photoaffinity.

INTRODUCTION

The hypoxia-inducible factor (HIF) is a basic helix–loop–helix heterodimeric transcription factor, composed of one of three subunits (HIF-1α, -2α, or -3α) and a HIF-1β subunit [1–3]. Under aerobic conditions, HIF-1α is rapidly degraded via a 26S proteasome-dependent pathway, whereas under hypoxic conditions, HIF-1α is stabilized and translocated into the nucleus where it dimerizes with the constitutively expressed HIF-1α [4–7]. The HIF-1α/β dimer binds to specific nucleotide sequences (hypoxia-responsive elements, HREs) in the promoter of hypoxia-responsive genes such as vascular endothelial growth factor (VEGF), insulin-like growth factor, heme oxygenase-1, and inducible nitric oxide synthase [8,9]. Among the HIF-regulated genes, VEGF plays a pivotal role in pathological angiogenesis and tumor growth [10,11]; therefore, the inhibition of VEGF inducer HIF is recognized as an attractive

Pure Appl. Chem.* **84, 2183–2498 (2012). A collection of invited papers based on presentations at the 14th International Meeting on Boron Chemistry (IMEBORON-XIV), Niagara Falls, Canada, 11–15 September 2011.
‡Corresponding author

strategy for cancer therapy [8,12]. Our efforts have been focused on the development of HIF inhibitors [13–17] as anti-angiogenesis agents. Recently, we reported that carboranylphenoxyacetanilide GN26361 (**1**) induced a potent inhibitory effect on HIF-1α activation under hypoxic conditions [18]. In the present study, we clarified the action mechanism of **1** against HIF inhibition.

RESULTS AND DISCUSSION

Standard chemical biology techniques, including photoaffinity labeling, click conjugation, and biotinylation, are very useful tools for detecting target proteins of biologically active molecules having undefined action mechanisms [19–21]. Based on this approach, we designed and synthesized multifunctional molecular probes of **1** substituted with benzophenone to form covalent binding with a target protein by UV (photoaffinity labeling), and an acetylene moiety to conjugate with azide-linked fluorescence by click reaction (Fig. 1A). The probes of **1** (**2** and **3**) were synthesized from 4-ethynylphenoxyacetic acid **5** and aminobenzophenones **6a–c** (Scheme 1). To confirm whether the synthesized probes exhibit HIF inhibitory activity, we examined the effects of the probes on the hypoxia-induced activation of HIF in human cervical cancer cells HeLa by HRE reporter gene assay and immunoblot analysis. As shown in Figs. 1B,C, although the inhibitory effects of the probes against HIF transcriptional activity were decreased almost 10-fold compared with **1** (Fig. 1B), the reducing property of the probes on the HIF-1α protein level was parallel to that of **1** (Fig. 1C). These results support that boronic acid in **1** is an efficient functional group for HIF inhibition, a finding similar to the results of our previous study [18].

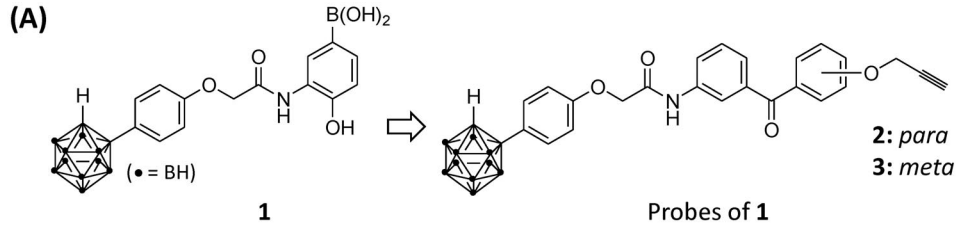

(B)

Compound	HRE Reporter Gene Assay IC_{50} (μM)
1	0.7±0.2
2	7.9±2.1
3	7.8±0.2

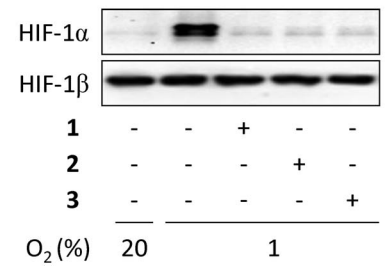

Fig. 1 Probes of carboranylphenoxy acetanilide **1** and their HIF inhibitory activity under hypoxic conditions. (A) Probes of **1**. (B) Inhibitory effects of **1** and probes on transcriptional activity of HIF were determined by HeLa cell-based HRE reporter gene assay. (C) Effects of **1** (10 μM) and probes (30 μM) on the hypoxia-induced increase in HIF-1α protein were determined by immunoblot in HeLa cells.

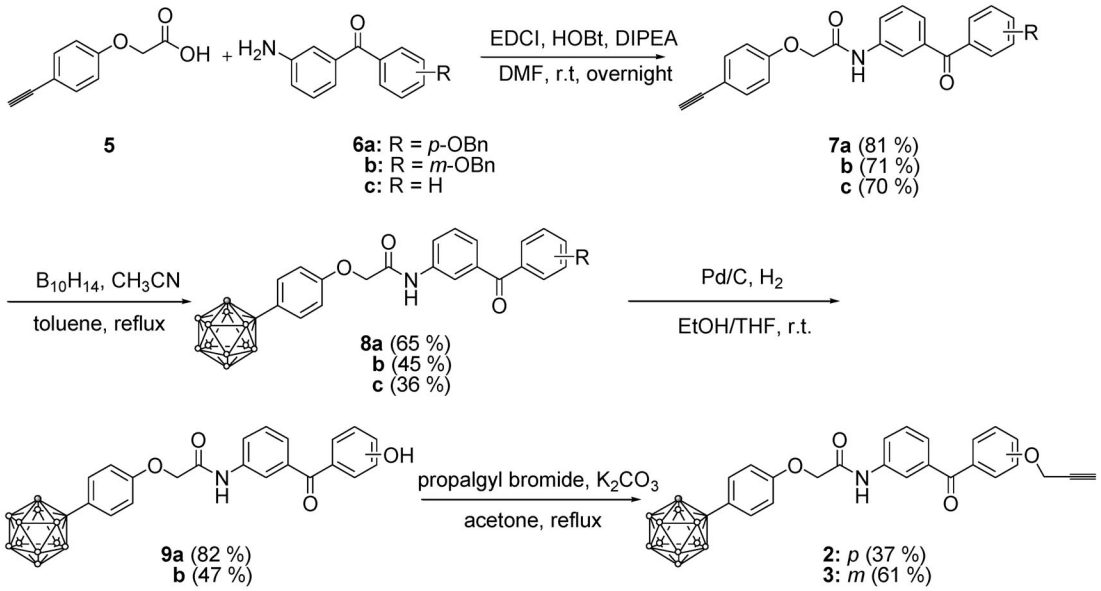

Scheme 1 Synthesis of molecular probes **2** and **3**.

Using these probes, we performed photoaffinity labeling in HeLa cell lysate and click conjugation with Alexa Fluor 488-azide to visualize the target protein. Following sodium dodecyl sulfate polyacrylamide gel electrophoresis (SDS-PAGE), proteins bound to the probe-Alexa Fluor 488 were visualized by direct in-gel fluorescence detection. As shown in Fig. 2A, a major fluorescent band above the

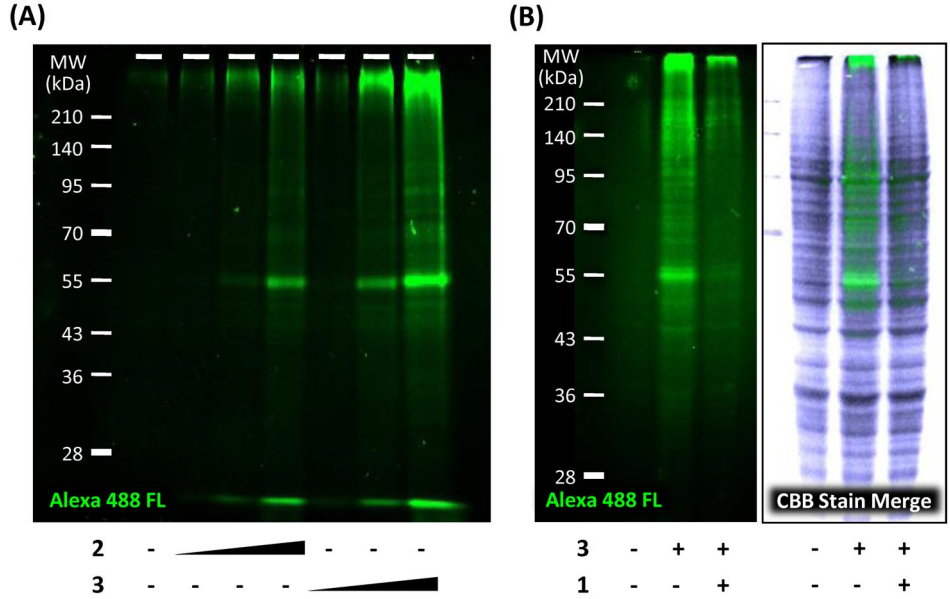

Fig. 2 Fluorescence imaging of target protein bound to the probe. (A) HeLa cell lysate was irradiated for 30 min at 360 nm with various concentrations (30, 100, and 300 μM) of each probe. The conjugation of probe and Alexa Flour 488-azide was performed by click reaction. (B) Total cell lysates from HeLa cells were photoaffinity-labeled with **3** (100 μM) in the presence or absence of **1** (500 μM).

55 kDa molecular weight marker was detected by both probes in a concentration-dependent manner, and binding of **3** with the protein was slightly more sensitive than that of **2**. To confirm the specificity of probe binding, we performed competition assays with **1** or **8c**, an acetylene-free analog of **2** and **3**. As shown in Fig. 2B, competition with **1** resulted in almost complete abrogation of the level of the fluorescent band at ~55 kDa. Furthermore, whole cell lysates from HeLa cells exposed to normoxic or hypoxic conditions (4 h) were preincubated with **8c**, and then photoaffinity was labeled with **3**. In both normoxic and hypoxic conditions, the band was decreased by the presence of **8c** (Fig. 3D, lanes 3 and 6). These results raise the possibility that the band at ~55 kDa may be the main target protein of **1** and its probes.

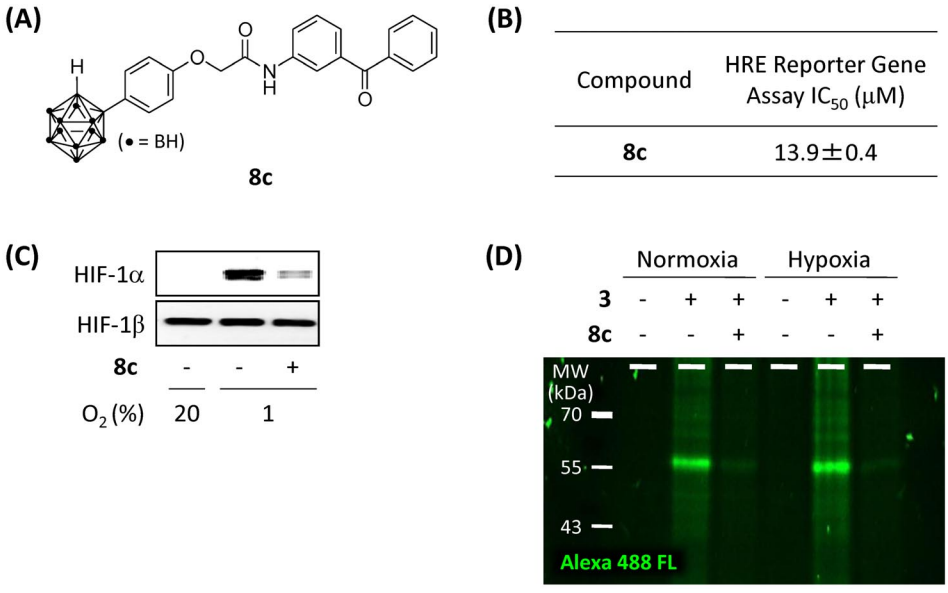

Fig. 3 HIF inhibitory activity of **8c**. (A) Structure of **8c**, an acetylene-free analog of **2** and **3**. (B) Inhibitory effects of 8c on transcriptional activity of HIF were determined by HeLa cell-based HRE reporter gene assay. (C) Effects of **8c** (30 μM) on the hypoxia-induced increase in HIF-1α protein were determined by immunoblot in HeLa cells. (D) Total cell lysates from HeLa cells incubated under normoxic or hypoxic condition (4 h) were photoaffinity-labeled with **3** (100 μM) in the presence or absence of **8c** (1 mM).

To identify the protein manifest at above 55 kDa, we next performed two-dimensional electrophoresis followed by in-gel digestion and peptide mass fingerprinting analysis (PMF) by liquid chromatography/electrospray ionization time-of-flight mass spectrometry (LC/ESI-TOF MS) (Fig. 4).

As shown in Table 1, PMF analysis searched in Mascot revealed that the protein bound to the probe was heat shock protein (HSP) 60 with a significant score value of 245, sequence coverage of 73 %, and 28 peptides matching. To confirm the direct binding of **3** and HSP60, in-gel fluorescence imaging was performed with recombinant human HSP60 protein, and a fluorescent band was observed in the presence of **3** (Fig. 5A, lane 2). Under these conditions, an excess of **1** suppressed the binding of HSP60 and **3** (Fig. 5A, lane 3). In addition, **3** selectively bound to HSP60 in mixture of recombinant HSP60, 70, and 90 (Fig. 5B). Moreover, the immunoprecipitation assay demonstrated that HSP60 interacts with HIF-1α in HeLa cells (Fig. 5C). These results suggest that the binding of **1** to HSP60 appears to be implicated in the inhibition of HIF-1α.

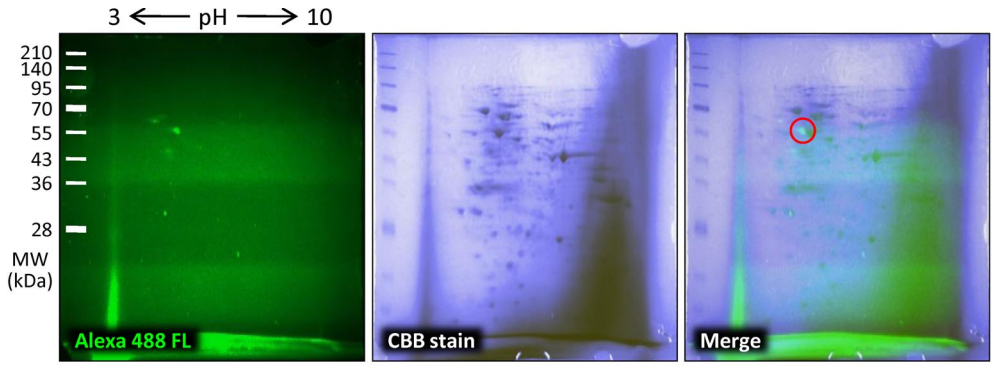

Fig. 4 Two-dimensional electrophoresis and fluorescent imaging. HeLa cell lysate was irradiated for 30 min at 360 nm with **3** (100 μM), and the conjugation of probe and Alexa Flour 488-azide was performed by click reaction. After dehydration of IPG strips containing the probe-labeled protein, isoelectric focusing was carried out. Alexa Fluor 488 fluorescence was visualized, and then the gel was stained with CBB.

Table 1 Results of mass spectrometric analysis.

Residues	MH^+ (observed)	Mr (calculated)	Sequence in HSP60
1–3	419.2325	418.2362	-.MLR.L
83–87	575.3318	574.3326	K.SIDLK.D
517–523	743.4327	742.4225	K.GIIDPTK.V
463–469	785.5008	784.5058	K.IGIEIIK.R
353–359	821.3976	820.4000	K.DDAMLLK.G Oxidation (M)
474–481	844.5019	843.4888	K.IPAMTIAK.N
397–405	901.5222	900.5280	K.LSDGVAVLK.V
293–301	912.5751	911.5804	K.VGLQVVAVK.A
421–429	960.4981	959.5036	R.VTDALNATR.A
482–493	1215.6408	1214.6507	K.NAGVEGSLIVEK.I
406–417	1233.5781	1232.5885	K.VGGTSDVEVNEK.K
61–72	1344.6934	1343.7085	R.TVIIEQSWGSPK.V
222–233	1389.6812	1388.6976	R.GYISPYFINTSK.G
143–156	1444.7790	1443.8007	R.GVMLAVDAVIAELK.K Oxidation (M)
206–218	1504.7285	1503.7490	K.TLNDELEIIEGMK.F
237–249	1601.7229	1600.7443	K.CEFQDAYVLLSEK.K
430–446	1684.8743	1683.8978	R.AAVEEGIVLGGGCALLR.C
555–573	1754.5677	1753.5875	K.DPGMGAMGGMGGGMGGGMF.- 5 Oxidation (M)
447–462	1771.8236	1770.8458	R.CIPALDSLTPANEDQK.I
251–268	1919.0358	1918.0636	K.ISSIQSIVPALEIANAHR.K
371–387	2037.9844	2037.0153	R.IQEIIEQLDVTTSEYEK.E
38–58	2129.0876	2128.1272	R.ALMLQGVDLLADAVAVTMGPK.G Oxidation (M)
38–58	2145.0866	2144.1221	R.ALMLQGVDLLADAVAVTMGPK.G 2 Oxidation (M)
269–290	2365.2883	2364.3264	R.KPLVIIAEDVDGEALSTLVLNR.L
527–551	2482.3555	2481.3942	R.TALLDAAGVASLLTTAEVVVTEIPK.E
494–516	2556.0468	2555.0866	K.IMQSSSEVGYDAMAGDFVNMVEK.G 3 Oxidation (M)
97–121	2560.2078	2559.2413	K.LVQDVANNTNEEAGDGTTTATVLAR.S
315–344	3113.4500	3112.5023	K.DMAIATGGAVFGEEGLTLNLEDVQPHDLGK.V Oxidation (M)

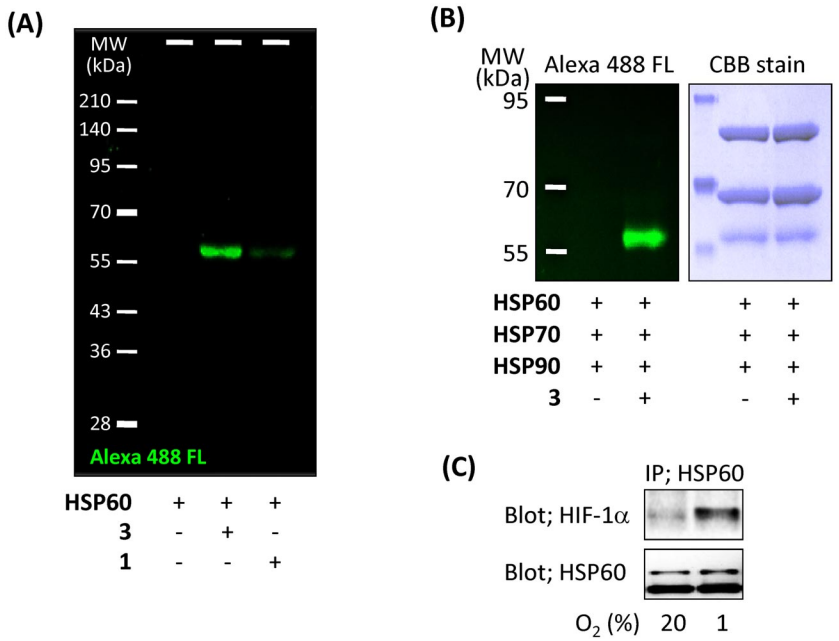

Fig. 5 Fluorescence imaging of probe-labeled recombinant HSP60, and interaction of HSP60 and HIF-1α. (A) Recombinant human HSP60 (2 μg) was irradiated with **3** (10 μM) in the presence or absence of **1** (100 μM), and click conjugated with Alexa Fluor 488-azide. (B) Recombinant human HSP60 (3.9 μg), HSP70 (4.7 μg), and HSP90 (5.9 μg) were irradiated with **3** (10 μM) and click-conjugated with Alexa Fluor 488-azide. (C) HeLa cell lysate was immunoprecipitated with anti-HSP60 antibody and immunoblotted with anti-HIF-1α or HSP60 antibody.

To further clarify the relationship between HSP60 and HIF-1α, the effects of a known HSP60 inhibitor epolactaene *tert*-butyl ester (ETB) **4** [22] (Fig. 6A) on the hypoxia-induced activation of HIF were examined. As shown in Fig. 6, **4** inhibited the hypoxia-induced accumulation of HIF-1α similar to **1** (Fig. 6B) and transcriptional activation of HIF with an IC_{50} value of 1.9 μM (Fig. 6C). Furthermore, **4** showed the competitive property against binding of **3** to recombinant HSP60 (Fig. 6D, lane 3). These results indicate that HSP60 inhibitor **4** inhibits activation of HIF as well as **1**, and support that HSP60 is involved in the activation of HIF-1α. Moreover, **1** inhibited HSP60 chaperone activity similar to **4** (Fig. 7A). Interestingly, **1** suppressed HSP60 ATPase activity (Fig. 7B), however, **4** did not affect.

It has been reported that HIF-1α is one of the client proteins of molecular chaperon HSP90, and geldanamycin, a HSP90 inhibitor that stimulates HIF-1α degradation by affecting folding and maturation [23–25]. Unlike HSP90, the interaction of HSP60 and HIF-1α has not been established. To our knowledge, this is the first report demonstrating the implication of HSP60 in HIF activation. However, details of the functional association between HSP60 and HIF-1α remain to be elucidated.

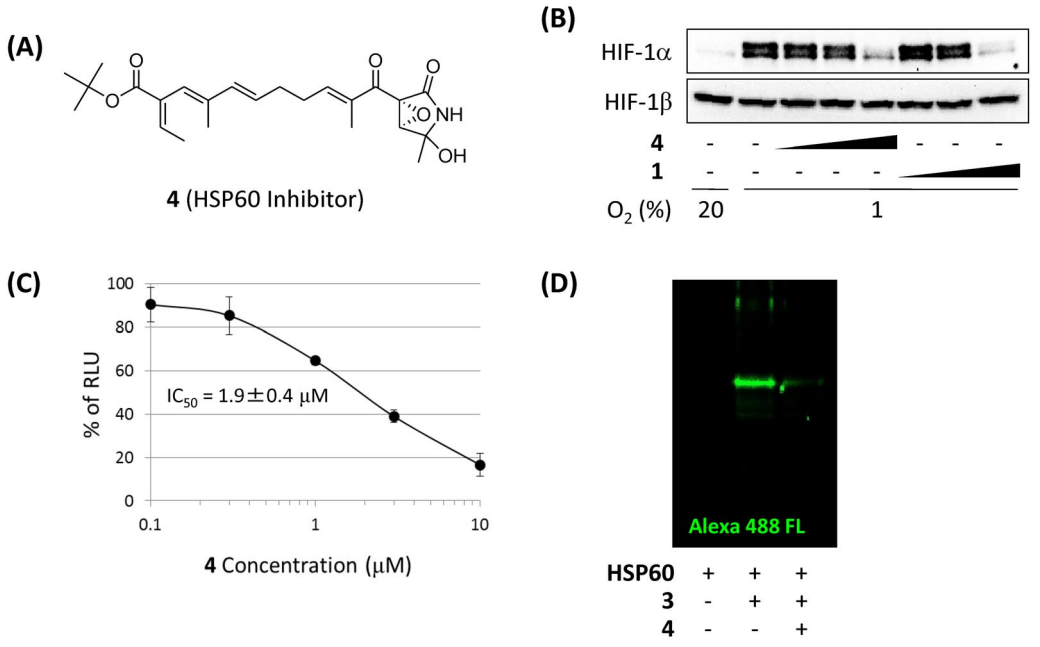

Fig. 6 HSP60 inhibitor suppresses HIF activation. (A) Structure of HSP60 inhibitor **4**. (B) HeLa cells were treated with various concentrations of **4** or **1** (0.1, 1, and 10 μM) under hypoxic condition. The protein levels of HIF-1α and -1β were detected by each specific antibody. (C) Inhibition of HIF transcriptional activity by **4** in HeLa cells. (D) Recombinant human HSP60 (2 μg) was irradiated with **3** (10 μM) in the presence or absence of **4** (100 μM), and click-conjugated with Alexa Fluor 488-azide.

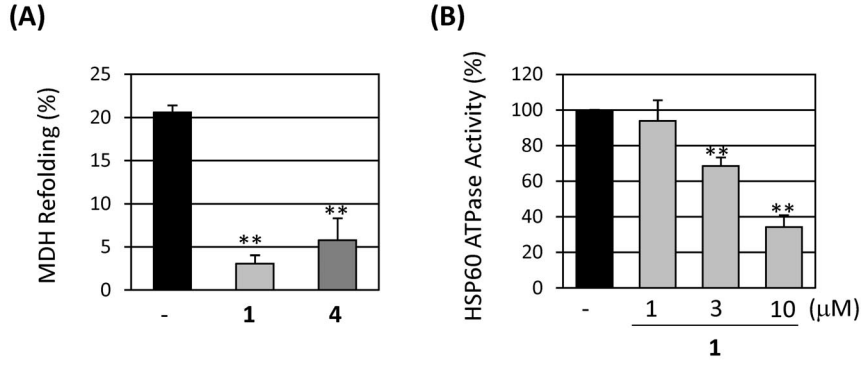

Fig. 7 Inhibition of HSP60 chaperone and ATPase activity by **1**. (A) Thermal aggregation of MDH was performed in the presence or absence of reconstituted HSP60 and HSP10. The level of MDH refolding by HSP60 and HSP10 was inhibited by **1** (10 μM) and **4** (10 μM). (B) HSP60 (1 μM) was incubated with or without **1**, and then treated with ATP (1 μM). After incubation for 30 min at 37 °C, ATP content was determined by luciferase/luciferin reaction.

CONCLUSION

We have succeeded in the design and synthesis of multifunctional molecular probes of HIF-1 inhibitor carboranylphenoxy acetanilide **1** for combining photoaffinity labeling and click reaction to identify the target protein. Using the probe, we identified that HSP60 was the target protein of **1**. Furthermore,

HSP60 inhibitor **4** suppressed hypoxia-induced HIF activation, indicating that HSP60 might be a new molecular target for HIF inhibition.

EXPERIMENTAL

General information

^{1}H and ^{13}C NMR spectra were recorded on JEOL JNM-AL 300 (300 MHz) or VARIAN UNITY-INOVA 400 (400 MHz) spectrometers. The chemical shifts are reported in δ units relative to internal tetramethylsilane. IR spectra were recorded on a Shimadzu FTIR-8200A spectrometer. High-resolution mass spectra (ESI) were recorded on a Bruker Daltonics micro TOF-15 focus. Elemental analyses were performed by a CE instrument EA1110 CHNS-O automatic elemental analyzer. Analytical thin layer chromatography (TLC) was performed on glass plates of silica gel 60 GF_{254} (Merck). Column chromatography was conducted on silica gel (Merck Kieselgel 70–230 mesh). Most commercially supplied chemicals were used without further purification.

Synthesis of chemical probes of 1

Synthesis of **2** and **3** is shown in Scheme 1. The carboxylic acid **5**, which was prepared according to our reported procedure [18], was reacted with the aminobenzophenones **6a** (*p*-isomer) or **6b** (*m*-isomer) using 1-(3-dimethylaminopropyl)-3-ethylcarbodiimide hydrochloride (EDCI) and l-hydroxybenzotriazole (HOBt) to give the corresponding aryloxyacetanides **7a** and **7b** in 81 and 71 % yields, respectively. Diisopropylethylamine (DIPEA) was an effective base for these amide formations. Decaborane coupling reaction proceeded at the ethynyl moiety of compounds **7** in the presence of acetonitrile as a Lewis base under toluene reflux to give the corresponding carborane derivatives **8a** and **8b** in 65 and 45 % yields, respectively. Debenzylation of compounds **8** was carried out in the presence of Pd/C under hydrogen atmosphere, and the resulting phenols were treated with propargyl bromide under basic conditions to afford the *m*-probe **2** and *p*-probe **3** in 37 and 61 % yields, respectively.

N-[3-(4-Benzyloxybenzoyl)phenyl]-2-(4-ethynylphenoxy)acetamide (7a)

To a mixture of 4-ethynylphenoxyacetic acid **5** (0.123 g, 0.7 mmol), 3-aminobenzophenone **6a** (0.19 g, 0.63 mmol), and DIPEA (0.12 mL, 0.7 mmol) in DMF (5.0 mL) were added EDCI (0.202 g, 1.0 mmol) and HOBT (0.142 g, 0.9 mmol), and the mixture was stirred overnight at room temperature. The mixture was then extracted with EtOAc, and the combined organic layer was washed with 1N HCl, neutralized with saturated aqueous $NaHCO_3$, washed with brine, and dried over $MgSO_4$. The solvent was evaporated, and the residue was purified by silica gel column chromatography with hexane/EtOAc (5/1) to provide **7a** (0.238 g, 0.52 mmol, 81 %) as a white solid: ^{1}H NMR (400 MHz; $CDCl_3$) δ 8.35 (bs, 1H), 7.98 (d, J = 8.4 Hz, 1H), 7.81–7.85 (m, 3H), 7.35–7.53 (m, 9H), 7.05 (d, J = 8.8 Hz, 2H), 6.95 (d, J = 8.8 Hz, 2H), 5.16 (s, 2H), 4.63 (s, 2H), 3.04 (s, 1H); ^{13}C NMR (75 MHz; $CDCl_3$) δ 194.7, 165.9, 162.5, 157.0, 139.1, 136.7, 136.1, 133.9, 132.5, 129.9, 129.0, 128.7, 128.2, 127.4, 126.2, 123.5, 121.0, 116.3, 114.7, 114.5, 82.9, 70.1, 67.4, 29.6; IR (KBr) 3286.5, 1697.2, 1542.9, 1434.9, 1380.9, 1249.8, 1172.6, 833.2, 698.2 cm^{-1}; HRMS (ESI, positive) *m/z* calcd. for $C_{30}H_{23}NO_4$ $[M+Na]^+$: 484.1525, found: 484.1525.

N-[3-(3-Benzyloxybenzoyl)phenyl]-2-(4-ethynylphenoxy)acetamide (7b)

^{1}H NMR (400 MHz; $CDCl_3$) δ 8.34 (bs, 1H), 8.01 (d, J = 8.4 Hz, 1H), 7.85 (s, 1H), 7.33–7.54 (m, 12H), 7.21–7.23 (m, 1H), 6.95 (d, J = 8.8 Hz, 2H), 5.12 (s, 2H), 4.63 (s, 2H), 3.04 (s, 1H); ^{13}C NMR (75 MHz; $CDCl_3$) δ 207.1, 195.6, 165.9, 158.7, 157.0, 138.5, 138.4, 136.8, 136.4, 1323.9, 129.4, 129.1, 128.6,

128.1, 127.5, 126.5, 124.0, 123.0, 121.2, 119.9, 116.3, 115.3, 114.7, 82.8, 70.2, 67.4; IR (KBr) 3255.6, 2341.4, 1693.4, 1542.9, 1504.4, 1288.4, 1242.1 cm^{-1}; HRMS (ESI, positive) *m/z* calcd. for $C_{30}H_{23}NO_4$ $[M + Na]^+$: 484.1525, found: 484.1521.

N-(3-Benzoylphenyl)-2-(4-ethynylphenoxy)acetamide (7c)

^1H NMR (400 MHz; $CDCl_3$) δ 8.33 (bs, 1H), 8.02 (d, J = 8.0 Hz, 1H), 7.87 (s, 1H), 7.82 (d, J = 8.4, 2H), 7.61–7.47 (m, 7H), 6.95 (d, J = 8.8, 2H), 4.64 (s, 2H), 3.04 (s, 1H); ^{13}C NMR (100 MHz; $CDCl_3$) δ 196.0, 165.9, 157.0, 138.4, 137.1, 136.9, 133.9, 132.6, 130.0, 129.1, 128.3, 126.5, 124.1, 121.3, 116.2, 114.7, 82.9, 76.7, 67.4; IR (KBr) 3379.1, 3259.5, 2360.7, 1693.4, 1651.0, 1604.7, 1539.1, 1504.4, 1242.1, 1068.5 cm^{-1}; HRMS (ESI, positive) *m/z* calcd. for $C_{23}H_{17}NO_3$ $[M + Na]^+$: 378.1106, found: 378.1101.

N-[3-(4-Benzyloxybenzoyl)phenyl]-2-(4-carboranylphenoxy)acetamide (8a)

A mixture of decaborane (0.023 g, 0.19 mmol), **7a** (0.10 g, 0.17 mmol), CH_3CN (0.26 mL, 5.0 mmol) was dissolved in toluene (5 mL) and refluxed for 18 h under argon. The solvent was evaporated and the residue was purified by silica gel column chromatography with hexane/EtOAc (2/1) to provide **8a** (0.064 g, 0.11 mmol, 65 %) as a white solid: ^1H NMR (400 MHz; $CDCl_3$) δ 8.27 (bs, 1H), 8.00 (d, J = 7.6 Hz, 1H), 7.84 (d, J = 9.2 Hz, 2H), 7.79 (s, 1H), 7.35–7.53 (m, 9H) 7.05 (d, J = 9.2 Hz, 2H), 6.94 (d, J = 8.8 Hz, 2H), 5.16 (s, 2H), 4.63 (s, 2H), 3.90 (bs, 1H); ^{13}C NMR (75 MHz; $CDCl_3$) δ 194.7, 165.9, 162.5, 157.0, 139.1, 136.7, 133.9, 132.5, 129.0, 128.7, 128.2, 127.4, 126.2, 123.5, 121.0, 116.3, 114.7, 114.5, 82.9, 70.1, 67.4, 29.6; IR (KBr) 3390.6, 3062.7, 2596.0, 1647.1, 1596.9, 1512.1, 1434.9, 1253.6, 1172.6, 1076.2, 840.9 cm^{-1}; HRMS (ESI, negative) *m/z* calcd. for $C_{30}H_{32}B_{10}NO_4$ $[M - H]^-$: 578.3335, found: 578.3331.

N-[3-(3-Benzyloxybenzoyl)phenyl]-2-(4-carboranylphenoxy)acetamide (8b)

^1H NMR (400 MHz; $CDCl_3$) δ 8.27 (bs, 1H), 8.04 (d, J = 9.2 Hz, 1H), 7.83 (s, 1H), 7.34–7.54 (m, 12H), 7.21–7.24 (m, 1H), 6.94 (d, J = 8.8 Hz, 2H), 5.12 (s, 2H), 4.63 (s, 2H), 3.90 (bs, 1H); ^{13}C NMR (75 MHz; $CDCl_3$) δ 195.6, 165.6, 158.7, 157.9, 138.4, 136.8, 136.5, 129.7, 129.5, 129.2, 128.7, 128.2, 127.6, 127.5, 126.7, 124.1, 123.1, 121.1, 120.0, 115.5, 114.9, 101.3, 77.2, 70.2, 67.5, 60.7; IR (KBr) 3390.6, 2576.7, 1697.2, 1589.2, 1512.1, 1434.9, 1276.8, 1191.1, 1076.2, 837.0, 752.2, 694.3 cm^{-1}; HRMS (ESI, negative) *m/z* calcd. for $C_{30}H_{32}B_{10}NO_4$ $[M - H]^-$: 578.3335, found: 578.3331.

N-(3-Benzoylphenyl)-2-(4-carboranylphenoxy)acetamide (8c)

This compound was prepared from **7c** (70 mg, 0.2 mmol) and decaborane (29 mg, 0.24 mmol) and acetonitrile (0.3 mL, 6 mmol) by the same procedure as described for compound **8c**. White solid (34 mg, 0.072 mmol, 36 %): ^1H NMR (400 MHz; $CDCl_3$) δ 8.27 (1H, bs), 8.04 (1H, d, J = 7.6 Hz), 7.85 (1H, s), 7.82 (2H, d, J = 7.2 Hz), 7.64–7.47 (7H, m), 6.94 (2H, d, J = 9.2 Hz), 4.63 (2H, s), 3.90 (1H, s); ^{13}C NMR (75 MHz, $CDCl_3$) δ 196.0, 165.7, 157.9, 138.5, 137.2, 136.9, 132.8, 130.1, 129.7, 129.2, 128.4, 127.7, 126.8, 124.1, 121.2, 114.9, 67.5, 60.8; IR (KBr) 3391, 3051, 2565, 1686, 1589, 1512, 1431, 1281, 1246, 1196, 1076 cm^{-1}; HRMS (ESI, negative): *m/z* calcd. for $C_{23}H_{27}B_{10}NO_3$ $[M - H]^-$: 472.2916, found: 472.2917.

2-(4-Carboranylphenoxy)-*N*-[3-(4-prop-2-ynyloxybenzoyl)phenyl]acetamide (2)

A suspension of **8a** (0.165 g, 0.28 mmol) and 10 % Pd/C (0.1 g) in EtOAc (15 mL) was stirred at room temperature under H_2. After 11 h, the mixture was filtered through a Celite bed and the filtrate was concentrated under reduced pressure. The residue was purified by silica gel column chromatography with hexane/EtOAc (3/1) to provide **9a** (0.113 g, 0.23 mmol, 82 %) as a white solid: ^{1}H NMR (400 MHz; $CDCl_3$) δ 8.30 (bs, 1H), 7.95 (d, J = 7.6 Hz, 1H), 7.83 (s, 1H), 7.79 (d, J = 8.4 Hz, 1H) 7.46–7.54 (m, 4H) 6.89–6.96 (m, 4H), 5.97 (s, 2H), 4.63 (s, 2H), 3.90 (bs, 1H). To a mixture of **9a** (0.042 g, 0.087 mmol), K_2CO_3 (0.115 g, 0.83 mmol) in acetone (3 mL) was added propargyl bromide (10 µL, 0.13 mmol), and the mixture was refluxed overnight under argon. The precipitate in the reaction mixture was removed by filtration, and the solvent was evaporated. The residue was extracted with EtOAc twice, and the combined organic layer was washed with saturated aqueous NH_4Cl and brine, and dried over $MgSO_4$. The solvent was evaporated and the residue was purified by silica gel column chromatography with hexane/EtOAc (3/1) to provide **2** (0.017 g, 0.032 mmol, 37 %) as a white solid: ^{1}H NMR (400 MHz; $CDCl_3$) δ 8.27 (bs, 1H), 8.01 (d, J = 8.0 Hz, 1H), 7.86 (d, J = 8.8 Hz, 2H) 7.80 (s, 1H), 7.46–7.54 (m, 4H), 7.07 (d, J = 8.8 Hz, 2H), 6.94 (d, J = 9.2 Hz, 2H), 4.79 (s, 2H), 4.62 (s, 2H), 3.90 (bs, 1H), 2,57 (s, 1H); ^{13}C NMR (72 MHz; $CDCl_3$) δ 194.8, 165.8, 161.4, 158.1, 139.2, 137.0, 132.7, 130.6, 129.9, 129.2, 127.8, 126.6, 123.9, 121.2, 115.1, 114.777.9, 76.4, 67.7, 60.9, 56.1; IR (KBr) 3398.3, 3298.0, 3062.7, 2596.0, 1596.9, 1512.1, 1434.9, 1303.8, 1253.6, 1176.5, 1076.2, 1022.2, 840.9 cm^{-1}; HRMS (ESI, negative) *m/z* calcd. for $C_{26}H_{28}B_{10}NO_4$ [M – H]$^-$: 526.3022, found: 526.3019.

2-(4-Carboranylphenoxy)-*N*-[3-(3-prop-2-ynyloxybenzoyl)phenyl]acetamide (3)

^{1}H NMR (400 MHz; $CDCl_3$) δ 8.33 (bs, 1H), 8.03 (d, J = 8.0 Hz, 1H), 7.85 (s, 1H), 7.41–7.58 (m, 7H), 7.22–7.26 (m, 1H), 6.94 (d, J = 8.8 Hz, 2H), 4.75 (s, 2H), 4.62 (s, 2H), 3.92 (bs, 1H), 2,54 (s, 1H); ^{13}C NMR (72 MHz; $CDCl_3$) δ 199.5, 195.4, 165.6, 157.8, 157.4, 138.4, 138.2, 136.8, 129.6, 129.4, 129.1, 127.5, 126.7, 124.2, 123.5, 121.2, 119.8, 115.6, 114.8, 78.0, 75.9, 67.4, 60.7, 55.9; IR (KBr) 3386.8, 3058.9, 2576.7, 1654.8, 1589.2, 1512.0, 1434.9, 1284.5, 1076.2, 837.0, 748.3, 682.8, cm^{-1}; HRMS (ESI, negative) *m/z* calcd. for $C_{26}H_{28}B_{10}NO_4$ [M – H]$^-$: 526.3022, found: 526.3023.

Cell culture

The human cervical carcinoma cell line HeLa cells were obtained from the Cell Resource Center for Biomedical Research, Institute of Development, Aging and Cancer, Tohoku University (Sendai, Japan). The cells were cultured at 37 °C under 5 % CO_2 atmosphere in RPMI 1640 medium (Wako Pure Chemicals, Osaka, Japan) supplemented with 10 % fetal bovine serum (FBS, HyClone, Logan, UT), 100 U/ml penicillin, and 100 µg/ml streptomycin (Invitrogen, Carlsbad, CA). For subsequent experiments, the cells were seeded at a density of 2×10^5 cells/ml/well in a 12-well TC plate (Greiner Japan, Tokyo, Japan), and incubated at 37 °C for 20 h. Hypoxic condition was achieved by replacing cells to 1 % O_2, 94 % N_2, and 5 % CO_2 in a multigas incubator (Astec, Fukuoka, Japan).

Immunoblotting and immunoprecipitation

After drug treatment for 4 h, the cells were washed three times with PBS (Ca/Mg-free), dipped in 100 µl of ice-cold lysis buffer (20 mM HEPES, pH 7.4, 1 % Triton X-100, 10 % glycerol, 1 mM EDTA, 5 mM sodium fluoride, 2.5 mM *p*-nitrophenylene phosphate, 10 µg/ml phenylmethylsulfonylfluoride, 1 mM sodium vanadate, and 10 µg/ml leupeptin) for 15 min, and disrupted with a Handy Sonic Disrupter, and the lysate was boiled for 5 min in a sample buffer (50 mM Tris, pH 7.4, 4 % SDS, 10 % glycerol, 4 % 2-thioethanol, and 50 µg/ml bromophenol blue) at a ratio of 4:1. The cell lysates were subjected to SDS-

PAGE, transferred to polyvinylidene difluoride (PVDF) membrane (GE Healthcare, Buckinghamshire, UK), and immunoblotted with anti-HIF-1α antibody and anti-HIF-1β antibody (BD Transduction Laboratories, Lexington, KY). After further incubation with horseradish peroxidase (HRP)-conjugated secondary antibody, the blot was treated with ECL kit (GE Healthcare) and protein expression was visualized with a Molecular Imager ChemiDoc XRS System (Bio-Rad, Hercules, CA). For immunoprecipitation, HeLa cells (2×10^6 cells) were dipped in 500 µl of ice-cold lysis buffer for 30 min at 4 °C. The lysis buffer containing the cells was centrifuged for 20 min at 13 200 rpm and 4 °C, and the supernatant obtained was incubated overnight at 4 °C with primary antibody (2 µg) with 20 µl Protein A/G plus-Agarose (Santa Cruz Biotechnology, Santa Cruz, CA).

Reporter-gene assay

HeLa cells expressing HRE-dependent luciferase reporter construct (HRE-Luc) were established with Cignal™ Lenti Reporter (SABiosciences, Frederick, MD) according to the manufacturer's instructions. The consensus sequence of HRE was 5'-TACGTGCT-3' from erythropoietin gene. Cells stably expressing the HRE-reporter gene were selected with puromycin. The cells were incubated for 12 h with or without drugs under the normoxic or hypoxic condition. After removal of the supernatant, the luciferase assay was performed using a Luciferase Assay System (Promega Corp., Madison, WI) according to the manufacturer's instructions.

Photoaffinity labeling, click chemistry, and fluorescent gel imaging

Soluble extract of HeLa cells was prepared using glass beads disruption in lysis buffer by centrifugation at 13 200 rpm for 20 min. The cell lysate (200 µg) or recombinant human HSP60 protein (2 µg, Assay Designs, Ann Arbor, MI) were incubated for 10 min at 4 °C with various concentrations of probe in the presence or absence of **1**, and then irradiated with 360 nm UV light (long-wave UV lamp model B-100A, UVP, Upland, CA) on ice for 30 min. Click reactions of probe and Alexa Fluor 488 azide [Alexa Fluor 488 5-carboxamide-(6-azidohexanyl), bis(triethylammonium salt), Invitrogen] were established with Click-iT Protein Reaction Buffer Kit (Invitrogen) according to the manufacturer's instructions. After the click reaction, proteins were precipitated with methanol/chloroform/water (60/15/40, v/v) and denatured by boiling for 5 min in a sample buffer. Proteins were separated by SDS-PAGE, and fluorescence of Alexa Fluor 488 was visualized in-gel using a Molecular Imager ChemiDoc XRS System.

Two-dimensional electrophoresis and proteomics

The dehydration of IPG strips (Immobiline DryStrip, pH 3–10, 7 cm, GE Healthcare) were performed for 12 h in dehydration buffer (8 M urea, 2 % CHAPS, 18 mM DTT, 2 % IPG buffer (GE Healthcare), and 50 µg/ml bromophenol blue) containing the probe-labeled protein. Isoelectric focusing was carried out as follows; 300 V for 4 h, 1000 V for 30 min, 5000 V for 80 min, and 5000 V for 25 min using the Ettan IPGphor 3 (GE Healthcare). The IPG strips were incubated for 15 min in equilibration buffer I (50 mM Tris-HCl, pH 8.8 containing 2 % SDS, 6 M urea, 30 % glycerol, and 1 % DTT) followed by equilibration buffer II (2% SDS, 6 M urea, 30 % glycerol, and 2.5 % iodoacetamide in 50 mM Tris-HCl, pH 8.8) for 15 min. The strips were then transferred to 12 % polyacrylamide gel, and electrophoresis was performed at 125 V. After visualization of Alexa Fluor 488 fluorescence, the gel was stained with coomassie brilliant blue (CBB). The Alexa Fluor 488 fluorescence-visualized and CBB-stained spots were excised from the gel, reduced with 10 mM DTT, alkylated with 55 mM iodoacetamide, and trypsinized for 8 h at 37 °C. The digested peptide fragments were analyzed by LC/ESI-TOF MS system (Bruker Daltonics, Bremen, Germany), and the PMF was performed against SwissProt database using Mascot (<www.matrixscience.com>).

MDH refolding assay

The chaperone activity of HSP60 was determined using malate dehydrogenase from porcine heart (MDH, Sigma) [22]. Denaturation of MDH (17.1 μM) was performed for 2 h at 25 °C in 10 mM HCl. A mixture of HSP60 (4 μM) and HSP10 (8 μM, Assay Designs) was incubated for 90 min at 30 °C with or without **1** or **4** in reconstitution buffer [50 mM Tris, pH 7.6, 300 mM NaCl, 20 mM KCl, 20 mM $Mg(CH_3COO)_2$ and 4 mM ATP]. The MDH folding reaction was performed in folding assay buffer (100 mM Tris, pH 7.6, 7 mM KCl, 7 mM $MgCl_2$, 10 mM DTT, and 2 mM ATP) and final concentrations of MDH, HSP60, and HSP10 were 1.71, 1, and 2 μM, respectively. After incubation for 30 min at 42 °C, aggregation of MDH was measured as the level of turbidity at 340 nm.

HSP60 ATPase assay

The human recombinant HSP60 (1 μM) was incubated for 30 min at 25 °C with or without various concentration of **1** in assay buffer (50 mM Tris, pH 7.6, 7 mM KCl, and 7 mM $MgCl_2$), and then treated with ATP (1 μM). After incubation for 30 min at 37 °C, ATP content was determined by luciferase/luciferin reaction (Promega).

ACKNOWLEDGMENT

This work was supported in part by a Grant-in-Aid for Scientific Research on Priority Areas "Cancer Therapy" from the Ministry of Education, Culture, Sports, Science and Technology, Japan.

REFERENCES

1. K. Iwai, K. Yamanaka, T. Kamura, N. Minato, R. C. Conaway, J. W. Conaway, R. D. Klausner, A. Pause. *Proc. Natl. Acad. Sci. USA* **96**, 12436 (1999).
2. A. L. Harris. *Nat. Rev. Cancer* **2**, 38 (2002).
3. P. H. Maxwell, M. S. Wiesener, G. W. Chang, S. C. Clifford, E. C. Vaux, M. E. Cockman, C. C. Wykoff, C. W. Pugh, E. R. Maher, P. J. Ratcliffe. *Nature* **399**, 271 (1999).
4. M. E. Cockman, N. Masson, D. R. Mole, P. Jaakkola, G. W. Chang, S. C. Clifford, E. R. Maher, C. W. Pugh, P. J. Ratcliffe, P. H. Maxwell. *J. Biol. Chem.* **275**, 25733 (2000).
5. E. Berra, D. E. Richard, E. Gothie, J. Pouyssegur. *FEBS Lett*. **491**, 85 (2001).
6. P. Jaakkola, D. R. Mole, Y. M. Tian, M. I. Wilson, J. Gielbert, S. J. Gaskell, A. Kriegsheim, H. F. Hebestreit, M. Mukherji, C. J. Schofield, P. H. Maxwell, C. W. Pugh, P. J. Ratcliffe. *Science* **292**, 468 (2001).
7. M. Ivan, K. Kondo, H. Yang, W. Kim, J. Valiando, M. Ohh, A. Salic, J. M. Asara, W. S. Lane, W. G. Kaelin Jr. *Science* **292**, 464 (2001).
8. G. L. Semenza. *Nat. Rev. Cancer* **3**, 721 (2003).
9. B. Dawn, R. Bolli. *Am. J. Physiol. Heart Circ. Physiol.* **289**, H522 (2005).
10. Y. Cao, P. Linden, J. Farnebo, R. Cao, A. Eriksson, V. Kumar, J. H. Qi, L. Claesson-Welsh, K. Alitalo. *Proc. Natl. Acad. Sci. USA* **95**, 14389 (1998).
11. N. Ferrara, H. P. Gerber, J. LeCouter. *Nat. Med.* **9**, 669 (2003).
12. G. L. Semenza. *Oncogene* **29**, 625 (2010).
13. A. Rapisarda, B. Uranchimeg, D. A. Scudiero, M. Selby, E. A. Sausville, R. H. Shoemaker, G. Melillo. *Cancer Res.* **62**, 4316 (2002).
14. M. Y. Koh, T. Spivak-Kroizman, S. Venturini, S. Welsh, R. R. Williams, D. L. Kirkpatrick, G. Powis. *Mol. Cancer Ther.* **7**, 90 (2008).
15. E.-J. Yeo, Y.-S. Chun, Y.-S. Cho, J. Kim, J.-C. Lee, M.-S. Kim, J.-W. Park. *J. Natl. Cancer Inst.* **95**, 516 (2003).

16. M. Uno, H. S. Ban, H. Nakamura. *Bioorg. Med. Chem. Lett.* **19**, 3166 (2009).
17. M.-S. Won, N. Im, S. Park, S. K. Boovanahalli, Y. Jin, X. Jin, K.-S. Chung, M. Kang, K. Lee, S.-K. Park, H. M. Kim, B. M. Kwon, J. J. Lee, K. Lee. *Biochem. Biophys. Res. Commun.* **385**, 16 (2009).
18. K. Shimizu, M. Maruyama, Y. Yasui, H. Minegishi, H. S. Ban, H. Nakamura. *Bioorg. Med. Chem. Lett.* **20**, 1453 (2010).
19. F. Kotzyba-Hibert, I. Kapfer, M. Goeldner. *Angew. Chem., Int. Ed.* **34**, 1296 (1995).
20. H. C. Kolb, M. G. Finn, K. B. Sharpless. *Angew. Chem., Int. Ed.* **40**, 2004 (2001).
21. V. V. Rostovtsev, L. G. Green, V. V. Fokin, K. B. Sharpless. *Angew. Chem., Int. Ed.* **41**, 2596 (2002).
22. Y. Nagumo, H. Kakeya, M. Shoji, Y. Hayashi, N. Dohmae, H. Osada. *Biochem. J*. **387**, 835 (2005).
23. K. Gradin, J. McGuire, R. Wenger, I. Kvietikova, M. fhitelaw, R. Toftgard, L. Tora, M. Gassmann, L. Poellinger. *Mol. Cell. Biol.* **16**, 5221 (1996).
24. N. J. Mabjeesh, D. E. Post, M. T. Willard, B. Kaur, E. G. Van Meir, J. W. Simons, H. Zhong. *Cancer Res.* **62**, 2478 (2002).
25. J. S. Isaacs, Y. J. Jung, E. G. Mimnaugh, A. Martinez, F. Cuttitta, L. M. Neckers. *J. Biol. Chem.* **277**, 29936 (2002).

